

Nuclear Reactions of Astrophysical Interest Involving Light Nuclei

H. Oberhummer*, W. Balogh, V.D. Efros†, H. Herndl, R. Hofinger

Institute of Nuclear Physics, Technical University Vienna, Wiedner Hauptstr. 8–10, A–1040 Wien, Austria

Abstract. An introduction to nucleosynthesis, the creation of the elements in the big bang, in interstellar matter and in stars is given. The two-step process ${}^4\text{He}(2n,\gamma){}^6\text{He}$ and the reverse photodisintegration ${}^6\text{He}(\gamma,2n){}^4\text{He}$ involving the halo nucleus ${}^6\text{He}$ could be of importance in the α -process in type-II supernovae. The reaction rates for the above processes are calculated using three-body methods and show an enhancement of more than three orders of magnitude compared to the previous adopted value. Direct-capture calculations give similar values for the above reaction rates. Therefore, this method was also used to calculate the reaction rates of the two-step processes ${}^6\text{He}(2n,\gamma){}^8\text{He}$ and ${}^9\text{Li}(2n,\gamma){}^{11}\text{Li}$ and the reverse photodisintegration of ${}^8\text{He}$ and ${}^{11}\text{Li}$ that could be also of importance in the α -process.

1 Introduction

One of the main driving forces for the evolution of our universe are nuclear processes. These nuclear processes are responsible for the energy production in stars as well as for the production of the elements in our universe. The process of the creation of the elements is called nucleosynthesis. We have three different scenarios, where nucleosynthesis occurs: in the big bang (primordial nucleosynthesis), in interstellar space (interstellar nucleosynthesis) and in stars (stellar nucleosynthesis). The result of nucleosynthesis is reflected today by the observed elemental abundances in different objects (sun and other stars, planets, meteorites, interstellar matter, ...).

The light elements from hydrogen to lithium with mass numbers $A = 1$ to $A = 7$ were mainly synthesized in primordial nucleosynthesis. In interstellar nucleosynthesis primarily elements from lithium to boron with mass numbers

*E-mail address: ohu@ds1.kph.tuwien.ac.at

†Permanent address: Kurchatov Institute, Institute for General and Nuclear Physics, SU-123182 Moscow, Russia

$A = 6$ to $A = 11$ were produced. Finally, all the heavier elements from carbon to uranium (in the astrophysical jargon these elements are called metals) with mass numbers $A = 12$ to $A = 238$ were created in stellar nucleosynthesis. Even though the heavier elements amount to about only 1% of the total observed abundance they are obviously indispensable for our environment. Without stellar nucleosynthesis our universe would be a boring place with the two gases hydrogen and helium (with a negligible amount of lithium, beryllium and boron) and without all the elements necessary for the existence of life.

One of the essential inputs for the investigation of different astrophysical scenarios for nucleosynthesis are cross sections, astrophysical S-factors and reaction rates of nuclear reactions as well as half lives and decay rates of nuclear decays. These quantities are determined using different experimental facilities (accelerators, reactors, . . .). However, in many cases it is not possible to obtain the needed cross sections directly from experiments. This is due to the fact that astrophysically relevant reactions take place mainly at thermonuclear energies. These energies are mostly well below the Coulomb and/or centrifugal barrier, and in this region the cross sections are often too small for experimental determination. Furthermore, in nucleosynthesis often radioactive nuclei are involved, for which experimental information is only scarcely available. For nuclei far-off stability often experimental information is not attainable at all.

In the next section a short introduction to nucleosynthesis is given emphasizing those astrophysical scenarios, where light nuclei are involved and methods developed in the few-body field could be applied. In Sect. 3 we show as an example for an application of few-body calculations for astrophysically relevant nuclear reactions the two-step process ${}^4\text{He}(2n,\gamma){}^6\text{He}$. This reaction involves also the halo nucleus ${}^6\text{He}$. In the last section we calculate the reaction rate for this reaction as well as other two-step reactions involving halo nuclei, like ${}^6\text{He}(2n,\gamma){}^8\text{He}$ and ${}^9\text{Li}(2n,\gamma){}^{11}\text{Li}$, using the simpler direct-capture (DC) model.

2 Nucleosynthesis

In this section we only can give a short introduction to nucleosynthesis. There are many textbooks where this subject can be found in more detail (e.g. [1]).

Primordial nucleosynthesis took place as the cooling early universe reached a temperature of about 10^9 K about three minutes after the big bang. Before that time the temperature was high enough that formed deuterons were immediately again destroyed through photodisintegration. From primordial nucleosynthesis calculations we can deduce abundance ratios of the light stable nuclides ${}^1\text{H}$, ${}^2\text{H}$, ${}^3\text{He}$, ${}^4\text{He}$, ${}^6\text{Li}$ and ${}^7\text{Li}$. Even some primordial abundance ratios may be altered somewhat by interstellar and stellar nucleosynthesis, the agreement between the abundances obtained from primordial nucleosynthesis with the observed abundances is remarkable.

In interstellar nucleosynthesis the nuclides ${}^6\text{Li}$, ${}^7\text{Li}$, ${}^9\text{Be}$, ${}^{10}\text{B}$ and ${}^{11}\text{B}$ are produced. In this scenario high-energy (larger than about 1 GeV) cosmic rays

hit interstellar matter and create through spallation processes the above nuclei.

Table 2.1. Nuclear burning phases and corresponding temperatures

| Nuclear burning phase | Temperature (T_9) |
|-----------------------|-----------------------|
| Hydrogen burning | 0.01–0.04 |
| Helium burning | 0.1–0.2 |
| Carbon burning | 0.6–0.8 |
| Neon burning | 1.2–1.4 |
| Oxygen burning | 1.5–2.2 |
| Silicon burning | 3–4 |

Stellar nucleosynthesis begins when through gravitational contraction in a star the density and temperature in the core gets high enough so that nuclear processes are ignited. Stellar nucleosynthesis takes place in successive burning phases. When the fuel of a preceding burning phase has been consumed, the ash of this burning phase is the fuel for the next burning phase. In the outer layers the previous burning phases still continue. The different burning phases are hydrogen burning (pp-chain, CNO-cycle, Ne–Na cycle, Mg–Al cycle), helium, carbon, neon, oxygen and silicon burning. In hydrogen burning helium is produced, in helium burning carbon and oxygen are synthesized, in the remaining advanced burning phases elements up to elements in the region of iron are produced. In successive burning phases the temperature must get larger, because of the increasing Coulomb barriers of the fusing heavier nuclei (Table 2.1).

The stars in which hydrogen burning takes place are named main-sequence stars, whereas the other burning phases occur in red giants. Not in all stars all the burning phases are ignited. For stars with less than approximately 8 solar masses, after helium burning, the outer part of the star that is blown off by strong stellar winds is called a planetary nebula, whereas the core remains as a white dwarf. For stars with more than about 8 solar masses all the above cited burning phases take place. Finally, after silicon burning the core of the star consists of elements with mass numbers in the region of iron. Then it is not possible to gain energy anymore through nuclear fusion and the star collapses. Through the rebound effect after the implosion the stellar mantle is ejected in a gigantic explosion, whereas the core remains as a neutron star or black hole. This dramatic event is called a supernova of type II (a supernova of type I takes place in a binary system consisting of two stars, where triggered through mass accretion from the accompanying star the star is disrupted completely).

There are astrophysical scenarios in which free neutrons play a dominating role. Most elements heavier than iron have been created through neutron capture in two processes: in the s-process occurring in helium burning of red giants and in the r-process occurring in a supernova of type II. The neutron flux in the s-process of helium burning is comparatively low ($N_n \simeq 10^8 \text{ cm}^{-3}$), whereas in the r-process it is much higher ($N_n \simeq 10^{20} \text{ cm}^{-3}$).

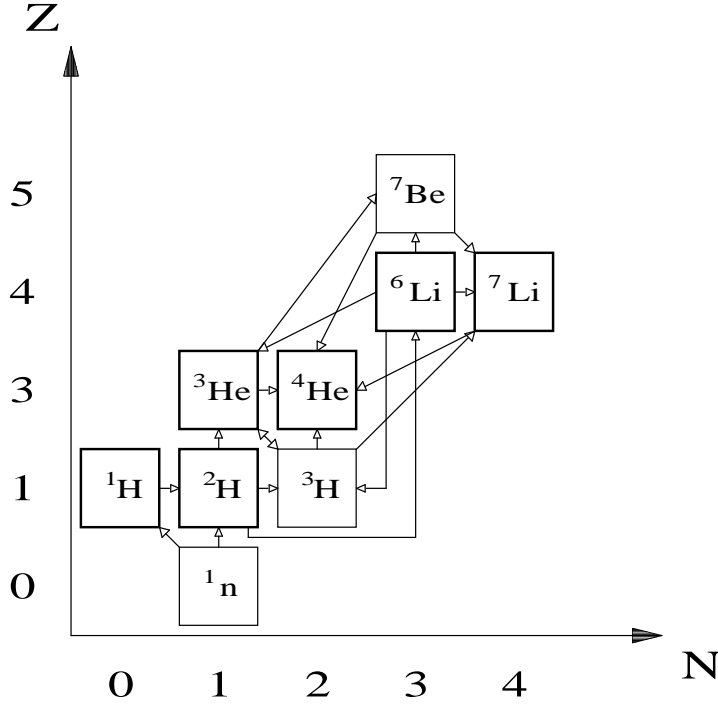


Figure 1. Primordial nucleosynthesis in the Standard Big Bang (SBB)

In Fig. 1 the nuclear reaction network for primordial nucleosynthesis in the Standard Big Bang (SBB) is shown. Fig. 2 shows the pp-chain dominating in low-mass main-sequence stars, like our sun, whereas the CNO-cycle takes over for more massive stars. There are two other scenarios additionally to the before discussed s- and r-process where neutron capture plays also a dominating role. The first one is an alternative to the standard Big Bang and is called the Inhomogenous Big Bang (IBB) with neutron densities up to about $N_n \simeq 10^{20} \text{ cm}^{-3}$. The second one is the so-called α -process occurring in type-II supernovae with neutron densities of about $N_n \simeq 10^{20-30} \text{ cm}^{-3}$. Fig. 3 shows the net-work up to a mass number of $A = 12$ which should be taken into account additionally to Fig. 2 for primordial nucleosynthesis in the IBB and the α -process. These are neutron-rich scenarios, where reactions involving light

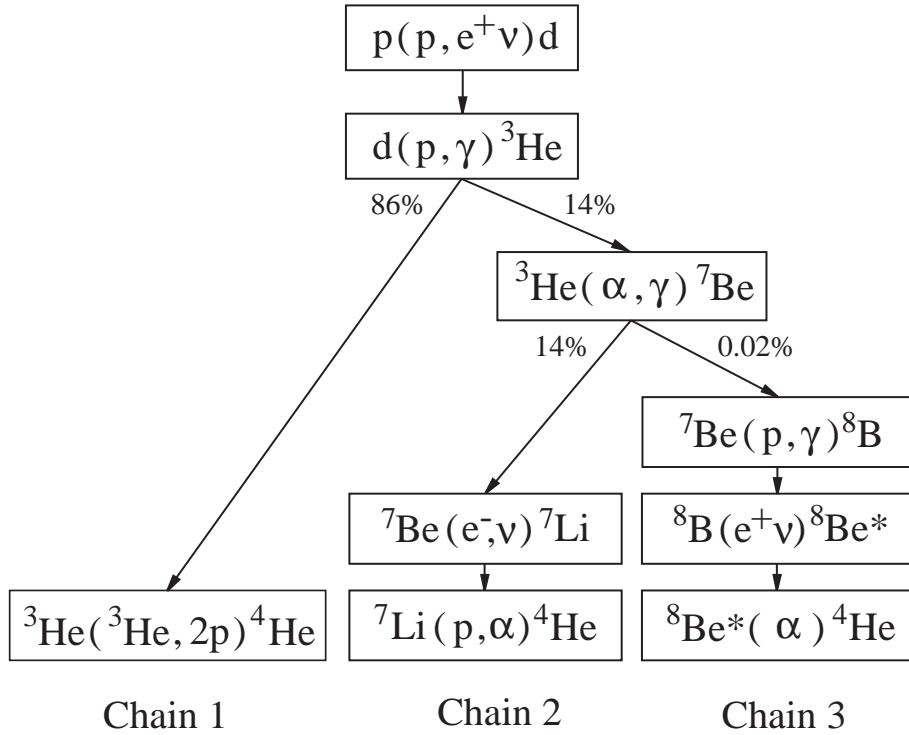


Figure 2. The pp-chain in hydrogen burning of main-sequence stars

nuclei on the neutron-rich side of the region of stability have to be included. The main nuclear reactions up to a mass number of $A = 12$ taking place in the SBB, IBB, pp-chain, helium burning and the α -process are listed in Table 2.2.

We want to discuss the α -process a little more, because the reaction rates calculated in the next section occur in this scenario. The α -process takes place in the neutrino-heated hot bubble between the nascent neutron star and the overlying stellar mantle of a type-II supernova [2, 3, 4, 5, 6]. During the gravitational collapse in the supernova the temperature in the core of the star gets so high (up to 10^{10} K) that all the nuclei are disassembled through photodissociation into protons and neutrons. Afterwards, the material being originally in nuclear statistical equilibrium (NSE) at high temperature, is expanded and cooled so rapidly that not all the α -particles have time to reassemble. In this environment most nucleons are either in the form of free neutrons or bound in α -particles. The nucleosynthesis in the neutrino bubble takes place in subsequent steps: first, α -particles are formed from the free nucleons. Then, in the following α -process, nuclei up to about $A \approx 100$ are produced [2]. Finally, the neutrino bubble is also an ideal site for the r-process synthesizing the elements of about $A \geq 100$ [2, 7, 8].

Table 2.2. Nuclear reactions of astrophysical interest for light nuclei up to $A = 12$. The left column lists the major reactions for nucleosynthesis in the Standard Big Bang (SBB), additional reactions in the pp-chain and helium burning. The right column lists reactions which can be additionally activated in the α -process or the Inhomogenous Big Bang (IBB).

| Target Nucleus | Residual Nucleus | Type of Reaction | Target Nucleus | Residual Nucleus | Type of Reaction |
|----------------|------------------|--|------------------------|------------------|--|
| SBB | | | α -process, IBB | | |
| ^1n | ^1H | β^- | ^4He | ^6He | $(2\text{n}, \gamma)$ |
| ^1H | ^2H | (n, γ) | ^6He | ^8He | $(2\text{n}, \gamma)$ |
| ^2H | ^3H | $(\text{n}, \gamma), (\text{d}, \text{p})$ | ^6He | ^6Li | β^- |
| ^2H | ^3He | $(\text{p}, \gamma), (\text{d}, \text{n})$ | ^6Li | ^{10}B | (α, γ) |
| ^2H | ^6Li | (α, γ) | ^7Li | ^8Li | (n, γ) |
| ^3H | ^3He | β^- | ^7Li | ^{11}B | (α, γ) |
| ^3H | ^4He | $(\text{d}, \text{n}), (\text{p}, \gamma)$ | ^7Be | ^8Be | (n, γ) |
| ^3H | ^7Li | (α, γ) | ^8He | ^8Li | β^- |
| ^3He | ^3H | (n, p) | ^8Li | ^9Li | (n, γ) |
| ^3He | ^4He | $(\text{d}, \text{p}), (\text{n}, \gamma)$ | ^8Li | ^8Be | β^- |
| ^3He | ^7Be | (α, γ) | ^8Li | ^{11}B | (α, p) |
| ^6Li | ^3H | (n, α) | ^8Be | ^9Be | (n, γ) |
| ^6Li | ^3He | (p, α) | ^9Li | ^9Be | β^- |
| ^6Li | ^7Li | (n, γ) | ^9Li | ^{11}Li | $(2\text{n}, \gamma)$ |
| ^6Li | ^7Be | (p, γ) | ^9Be | ^6Li | (p, α) |
| ^7Li | ^4He | (p, α) | ^9Be | ^{10}Be | (n, γ) |
| ^7Be | ^7Li | (e^-, ν) | ^9Be | ^{10}B | $(\text{p}, \gamma), (\text{d}, \text{n})$ |
| ^7Be | ^4He | (n, α) | ^9Be | ^{12}B | (α, p) |
| ^7Be | ^7Li | (n, p) | ^9Be | ^{12}C | (α, n) |
| pp-chain | | | ^{10}Be | ^{11}Be | (n, γ) |
| ^1H | ^2H | $(\text{p}, \text{e}^+ \nu)$ | ^{10}Be | ^{10}B | β^- |
| ^2H | ^3He | (p, γ) | ^{10}B | ^7Li | (n, α) |
| ^3He | ^4He | $(^3\text{He}, 2\text{p})$ | ^{10}B | ^{11}B | (n, γ) |
| ^3He | ^7Be | (α, γ) | ^{11}Li | ^{11}Be | β^- |
| ^7Be | ^8B | (p, γ) | ^{11}Be | ^{12}Be | (n, γ) |
| ^8B | ^8Be | β^+ | ^{11}Be | ^{11}B | β^- |
| ^8Be | $^4\text{He}^*$ | decay | ^{11}B | ^{12}B | (n, γ) |
| helium burning | | | ^{11}B | ^{12}C | $(\text{p}, \gamma), (\text{d}, \text{n})$ |
| ^4He | ^{12}C | $(2\alpha, \gamma)$ | ^{12}Be | ^{12}B | β^- |
| ^8Be | ^4He | decay | ^{12}B | ^{12}C | $\beta^-, (\text{p}, \text{n})$ |

3 Few-Body Calculations

Few-body methods have been used only partially for the calculation of astrophysical S-factors or reaction rates of astrophysically relevant nuclear reactions. An example is an exact three-nucleon calculation for radiative capture by deuterons starting from realistic NN-potentials. In this calculation the astrophysically relevant reaction rates for ${}^2\text{H}(p,\gamma){}^3\text{He}$ at thermonuclear energies and ${}^2\text{H}(n,\gamma){}^3\text{H}$ at thermal energies have been determined [9]. Another example is the calculation of the non-resonant part of the cross section for ${}^4\text{He}(d,\gamma){}^6\text{Li}$ in the thermonuclear energy region. It was calculated in an $\alpha+p+n$ model by solving the three-body Faddeev equations [10] and using a three-body variational approach in the asymptotic region [11].

In the following we present the two-step processes ${}^4\text{He}(2n,\gamma){}^6\text{He}$ and the photodisintegration of ${}^6\text{He}$ as an example for an application of few-body calculations to astrophysically relevant nuclear reactions. A more extensive presentation of this calculation is given in ref. [12].

The reaction rate per particle triplet for ${}^4\text{He}(2n,\gamma){}^6\text{He}$, in analogy to the triple-alpha process, is given by [13]

$$\langle 2n^4\text{He} \rangle = 2 \int_0^\infty dE_1 \frac{\hbar}{\Gamma({}^5\text{He}, E_1)} \frac{d\langle n^4\text{He} \rangle(E_1)}{dE_1} \int_0^\infty dE_2 \frac{d\langle n^5\text{He} \rangle(E_1, E_2)}{dE_2}, \quad (1)$$

where E_1 and E_2 are the relative energies in the $({}^4\text{He}+n)$ - and $({}^5\text{He}+n)$ -system, respectively. To determine the reaction rate in Eq. (1), an integration over both energies E_1 and E_2 has to be performed. The quantity $\Gamma({}^5\text{He}, E_1)$ is the energy-dependent width of ${}^5\text{He}$, whereas $d\langle n^4\text{He} \rangle(E_1)/dE_1$ and $d\langle n^5\text{He} \rangle(E_1, E_2)/dE_2$ are the integrands of the reaction rates $\langle \sigma v \rangle$ [1] for the first and second step, respectively.

To calculate the second step reaction rate $\langle n^5\text{He} \rangle$, the ${}^5\text{He}(n,\gamma){}^6\text{He}$ cross section is required. One may estimate that the electric dipole transition E1 from the incident s-wave is dominating the reaction. This is confirmed by both three-body and direct-capture calculations. The cross section is given by

$$\sigma_{\text{E1}}(E_1, E_2) = \frac{2\pi}{81} \left(\frac{E_\gamma}{\hbar c} \right)^3 \frac{e^2}{\hbar v_2} |I|^2 \quad (2)$$

with

$$I = \frac{1}{k_2} \int_0^\infty dr_1 \int_0^\infty dr_2 u_b(E_1, r_1) r_1 u_{\text{sc}}(E_2, r_2) r_2^2 f_{\ell=1, j=3/2}(r_1, r_2), \quad (3)$$

where $E_\gamma = E_1 + E_2 + Q_{12}$ is the energy of the photon, with Q_{12} being the Q-value of the reaction ${}^4\text{He}(2n,\gamma){}^6\text{He}$. In Eq. (3) the coordinates r_1 and r_2 are the distances of the valence neutrons from the α -core and ${}^5\text{He}$, respectively. The quantities v_2 and k_2 are the relative velocity and wave number in the entrance

Table 3.1. Relevant input parameters for our calculations: Q_{12} is the Q-value for both steps, J^{Π} , E_{R} and Γ_{R} are the spin-parity assignments, resonance energies and widths of the intermediate nuclei ${}^5\text{He}$, ${}^7\text{He}$ and ${}^{10}\text{Li}$

| reaction | Q_{12} [MeV] | J^{Π} | E_{R} [MeV] | Γ_{R} [MeV] |
|---|--------------------|---------------------------|----------------------|----------------------------|
| ${}^4\text{He}(2\text{n},\gamma){}^6\text{He}$ | 0.98 ^{a)} | $\frac{3}{2}^{-\text{b)}$ | 0.89 ^{b)} | $0.76 \pm 0.11^{\text{c)}$ |
| ${}^6\text{He}(2\text{n},\gamma){}^8\text{He}$ | 2.14 ^{a)} | $\frac{3}{2}^{-\text{b)}$ | 0.44 ^{b)} | $0.16 \pm 0.03^{\text{b)}$ |
| ${}^9\text{Li}(2\text{n},\gamma){}^{11}\text{Li}$ | 0.31 ^{a)} | 1^{+d) | 0.54 ^{d)} | $0.22 \pm 0.01^{\text{d)}$ |

^{a)} Ref. [17]; ^{b)} Ref. [18]; ^{c)} Ref. [19]; ^{d)} Ref. [20]

channel (${}^5\text{He}+\text{n}$) of the second step. The quantity $u_{\text{b}}(E_1, r_1)/r_1$ represents the radial part of the quasi-bound wave function of the ${}^5\text{He}$ -resonance, and $u_{\text{sc}}(E_2, r_2)/r_2$ is the radial part of the (${}^5\text{He}+\text{n}$)-scattering wave function. The function $f_{\ell=1, j=3/2}(r_1, r_2)$ is the radial component in the expansion

$$\Psi({}^6\text{He}) = \sum_{\ell j} f_{\ell j}(r_1, r_2) [\chi_{\ell j}(\hat{\mathbf{r}}_1, \sigma_{1z}) \chi_{\ell j}(\hat{\mathbf{r}}_2, \sigma_{2z})]_{J=0} \quad (4)$$

of the $\alpha+\text{n}+\text{n}$ ground-state wave function. Here $\chi_{\ell j}$ are the angular-momentum functions with orbital angular momentum ℓ and total angular momentum $j = \ell \pm 1/2$, and the brackets [...] denote vector coupling. The expansion includes only equal ℓ -values for both neutrons and only the ($\ell = 1, j = 3/2$)-component contributes to the cross section.

To calculate the first step reaction rate $\langle \text{n}^4\text{He} \rangle$ we need the (${}^4\text{He}+\text{n}$)-potential. It was obtained by fitting a folding-type potential [14, 15] to the experimental energy and width of the ${}^5\text{He}$ ground state. For the calculation of the energy dependent width $\Gamma({}^5\text{He}, E_1)$ of ${}^5\text{He}$ in Eq. (1) we used an equivalent square well potential with the same r.m.s. radius of the density distribution as for the folding potential.

In the second step the ground-state wave function $u_{\text{b}}(E_1, r_1)$ of ${}^5\text{He}$ was determined by solving the single-particle Schrödinger equation, using the (${}^4\text{He}+\text{n}$)-potential and a boundary condition for a decaying system. It was then cut at a reasonable cut-off radius. For the determination of the scattering wave function $u_{\text{sc}}(E_2, r_2)$ we used again folding-type potentials. An accurate three-body wave function of ${}^6\text{He}$ (see [16]) was used in our calculations.

The relevant input parameters for the calculations of the reaction rate are shown in Table 3.1. The calculated cross section for ${}^5\text{He}(\text{n},\gamma){}^6\text{He}$ can be parametrized by $\sigma = \sigma_1/(E_2 [\text{MeV}])^{1/2} [\mu\text{b}]$. The ${}^5\text{He}(\text{n},\gamma){}^6\text{He}$ cross section exhibits the well-known $1/v$ -behavior for incident s-waves.

The obtained reaction rate can be parametrized in the following way:

$$N_{\text{A}}^2 \langle 2\text{n}^4\text{He} \rangle = a T_9^b \exp\left(\frac{c}{T_9}\right) 10^{-8} \text{ cm}^6 \text{ s}^{-1} \text{ mol}^{-2} \quad , \quad (5)$$

where the parameters a, b, c are shown in Table 3.2 for the two temperature regions $0.1 \leq T_9 < 2$ and $2 \leq T_9 \leq 15$ (T_9 : in units of 10^9 K). The inverse

Table 3.2. Parameters of the cross section for ${}^5\text{He}(n,\gamma){}^6\text{He}$ and the reaction rates for ${}^4\text{He}(2n,\gamma){}^6\text{He}$ and the reverse photodisintegration of ${}^6\text{He}$ calculated in our three-body model and in direct capture

| | Three-body calculation | | Direct-capture calculation | |
|--|------------------------|-------------------|----------------------------|-------------------|
| σ_1 [MeV $^{1/2}$ μb] | 0.152 | | 0.270 | |
| | $0.1 \leq T_9 \leq 2$ | $2 < T_9 \leq 15$ | $0.1 \leq T_9 \leq 2$ | $2 < T_9 \leq 15$ |
| a | 0.00265 | 0.293 | 0.00471 | 0.520 |
| b | 2.55 | -0.351 | 2.55 | -0.351 |
| c | 0.181 | -5.24 | 0.181 | -5.24 |
| d | 3.14 | 0.0286 | 3.14 | 0.0286 |
| e | -1.05 | 1.85 | -1.05 | 1.85 |
| f | -21.9 | -16.5 | -21.9 | -16.5 |

reaction rate λ_γ per nucleus per second can be calculated by using the RevRatio [21]

$$\lambda_\gamma = \text{RevRatio} \times N_A^2 \langle 2n^4\text{He} \rangle \text{ s}^{-1} \quad , \quad (6)$$

where we assumed that the photodisintegration proceeds through the ${}^5\text{He}$ resonance. The RevRatio is parametrized in the following way

$$\text{RevRatio} = dT_9^e \exp\left(\frac{f}{T_9}\right) 10^{23} \text{ cm}^{-6} \text{ mol}^2 \quad . \quad (7)$$

The parameters d, e, f are also shown in Table 3.2.

The reaction rate for ${}^4\text{He}(2n,\gamma){}^6\text{He}$ calculated with the help of our three-body model (second column of Table 3.2) is at least more than three orders of magnitude larger than the previously adopted value [21]. This is mainly due to the non-resonant E1-transition of the second step ${}^5\text{He}(n,\gamma){}^6\text{He}$, which dominates the cross section, and which was not taken into account previously.

4 Direct-capture (DC) calculations

We also calculated the reaction rates for ${}^4\text{He}(2n,\gamma){}^6\text{He}$ and the reverse photodisintegration of ${}^6\text{He}$ by using the DC model for the second step of the reaction. In this case Eq. 3 reduces to

$$I = \frac{S_{\ell=1,j=3/2}}{k_2} \int_0^\infty dr u_{\text{sc}}(E_2, r) r^2 u_{\ell=1,j=3/2}(r) \quad , \quad (8)$$

where $r \equiv r_2$ and $S_{\ell=1,j=3/2}$ is the spectroscopic factor and $u_{\ell=1,j=3/2}(r)$ is the wave function for ${}^6\text{He} = {}^5\text{He}+n$.

The spectroscopic factor for ${}^5\text{He}(n,\gamma){}^6\text{He}$ was calculated by shell-model calculations using the (6-16) 2BME interaction of Cohen and Kurath [22] and is given by $S_{\ell=1,j=3/2} = 1.3139$. All the other parameters (see Table 3.1) for

Table 4.1. Parameters for the cross section of the second step and reaction rates of ${}^6\text{He}(2n,\gamma){}^8\text{He}$ and ${}^9\text{Li}(2n,\gamma){}^{11}\text{Li}$, and the reverse photodisintegration of ${}^8\text{He}$ and ${}^{11}\text{Li}$ calculated in direct capture

| | ${}^6\text{He}(2n,\gamma){}^8\text{He}$ | | ${}^9\text{Li}(2n,\gamma){}^{11}\text{Li}$ | |
|--------------------------------------|---|-------------------|--|-------------------|
| $\sigma_{1\text{MeV}} [\mu\text{b}]$ | 1.828 | | 0.2435 | |
| | $0.1 \leq T_9 \leq 2$ | $2 < T_9 \leq 15$ | $0.1 \leq T_9 \leq 2$ | $2 < T_9 \leq 15$ |
| a | 8.015 | 36.91 | 0.651 | 0.956 |
| b | -0.209 | -1.187 | 0.042 | -0.412 |
| c | -2.514 | -4.262 | -3.394 | -3.432 |
| d | 0.013 | 0.003 | 0.004 | 0.003 |
| e | 1.709 | 2.687 | 1.458 | 1.912 |
| f | -27.427 | -25.679 | -6.470 | -6.432 |

the DC calculation of ${}^4\text{He}(2n,\gamma){}^6\text{He}$ were assumed to be the same as in the three-body calculation. For the DC calculation we used the code TEDCA [23].

As can be seen from Table 3.2 the cross section for the second step and the total reaction rate of ${}^4\text{He}(2n,\gamma){}^6\text{He}$ is enhanced by 78% compared to the three-body calculations. Therefore, we assumed that the DC model is also adequate within a factor of two to calculate the reaction rates for two other two-step processes involving halo nuclei like ${}^6\text{He}(2n,\gamma){}^8\text{He}$ and ${}^9\text{Li}(2n,\gamma)$, and the photodisintegration of ${}^8\text{He}$ and ${}^{11}\text{Li}$. These reactions could also be of importance in the α -process.

We assume as for ${}^4\text{He}(2n,\gamma){}^6\text{He}$ that again two p-neutrons are transferred in the two-step process and that in the second step the E1-transition is dominating. For ${}^9\text{Li}(2n,\gamma){}^{11}\text{Li}$ we did not consider yet possible predicted low-energy intruder s-states in ${}^{10}\text{Li}$ [24, 20] and/or ${}^{11}\text{Li}$ [25, 26]. Such states could lead to s-wave resonances in ${}^{11}\text{Li}$ near the $({}^{10}\text{Li}+n)$ -threshold modifying our calculated non-resonant cross section for ${}^{10}\text{Li}(n,\gamma){}^{11}\text{Li}$. Furthermore, by considering such s-wave states the two-step process could also proceed over 1^- or 2^- -states in ${}^{10}\text{Li}$ and not only over the 1^+ -state at 0.54 MeV above threshold (see Table 3.1) that we considered in our DC-calculation.

The used input parameters are again shown in Table 3.1. The spectroscopic factors are given by $S_{\ell=1,j=3/2} = 3.2047$ for ${}^7\text{He}(n,\gamma){}^8\text{He}$, and $S_{\ell=1,j=3/2} = 0.647$ and $S_{\ell=1,j=1/2} = 0.024$ for ${}^{10}\text{Li}(n,\gamma){}^{11}\text{Li}$. For the potentials in the exit channels we used the folding method adjusted to the separation energy and the r.m.s. radii of the neutrons for the residual nuclei.

The results for the parameters of the cross sections for the second step and the reaction rates are also shown in Table 4.1. The reaction rate for ${}^6\text{He}(2n,\gamma){}^8\text{He}$ is at $T_9 \approx 1$ about a factor 40 larger than for ${}^4\text{He}(2n,\gamma){}^6\text{He}$. Very similar results for the reaction rate of ${}^4\text{He}(2n,\gamma){}^6\text{He}$ have also been obtained in another DC calculation by Görres et al. [27]. However, our reaction rate for ${}^6\text{He}(2n,\gamma){}^8\text{He}$ is more than a factor 10 larger than in ref. [27], mainly because we used a larger spectroscopic factor. The reaction rate for ${}^9\text{Li}(2n,\gamma){}^{11}\text{Li}$ (Ta-

ble 4.1) is at $T_9 \approx 1$ almost a factor two enhanced compared to ${}^4\text{He}(2n,\gamma){}^6\text{He}$ (Table 3.2), even though the total Q-value for the Li-reaction is a factor three smaller (Table 3.1). This is mainly due to the more pronounced halo structure of the Li-nuclei as compared to the He-nuclei.

Acknowledgement. The authors are indebted to I.J. Thompson for help in their work and to J.S. Vaagen and M.V. Zhukov for valuable discussions on halo nuclei. This work was supported by the Fonds zur Förderung der wissenschaftlichen Forschung in Österreich (project P10361-PHY), by the Österreichische Nationalbank (project 5054) and by the International Science Foundation (grant J4M100). Partial financial support by the Russian-British-Northic Theory collaboration (RNBT) is acknowledged.

References

1. C.E. Rolfs, W. Rodney: *Cauldrons in the Cosmos*. Chicago: University of Chicago Press 1988
2. S.E. Woosley, R.D. Hofmann: *Astrophys. J.* **395**, 202 (1992)
3. B.S. Meyer et al.: *Astrophys. J.* **399**, 656 (1992)
4. W.M. Howard et al.: *Astrophys. J.* **417**, 713 (1993)
5. S.E. Woosely et al.: *Astrophys. J.* **433**, 229 (1994)
6. J. Witti, H.-Th. Janka and K. Takahashi: *Astron. and Astrophys.* **286**, 841 (1994)
7. K.L. Kratz et al.: *Astrophys. J.* **403**, 216 (1993)
8. K. Takahashi, J. Witti and H.-Th. Janka: *Astron. and Astrophys.* **286**, 857 (1994)
9. J.L. Friar et al.: *Phys. Rev. Lett.* **66**, 1827 (1991)
10. L.D. Blokhintsev et al.: *Phys. Rev. C* **48**, 2390 (1993)
11. V.I. Kukulin et al.: *Nucl. Phys. A* **417**, 128 (1984); **453**, 365 (1986)
12. V.D. Efros et al.: *Phys. Lett. B* (submitted)
13. K. Nomoto, F.-K. Thielemann, S. Hiyaji: *Astron. and Astrophys.* **149**, 239 (1985)
14. A.M. Kobos et al.: *Nucl. Phys. A* **425**, 205 (1984)
15. H. Oberhummer, G. Staudt: In: H. Oberhummer, (ed.): *Nuclei in the Cosmos*, p.29. Heidelberg: Springer Verlag 1991
16. M.V. Zhukov et al.: *Physics Rep.* **231**, 151 (1993)

17. G. Audi, A.H. Wapstra: Nucl. Phys. A **565**, 1 (1993)
18. F. Ajzenberg-Selove: Nucl. Phys. A **490**, 1 (1988)
19. V.D. Efros et al.: Phys. Rev. C (to be submitted)
20. B.M. Young et al.: Phys. Rev. C **49**, 279 (1994)
21. W.A. Fowler, G.R. Caughlan and B. Zimmerman: Ann. Rev. Astron. Astrophys. **13**, 69 (1975)
22. S. Cohen, D. Kurath: Nucl. Phys. **73**, 1 (1965)
23. H. Krauss: Computer code TEDCA. Technical University Vienna, 1992
24. R. Kryger et al.: Phys. Rev. C **47**, R4239 (1993)
25. I.J. Thompson, M.V. Zhukov: Phys. Rev. C **49**, 1904 (1994)
26. S. Shimamura et al.: Phys. Lett. B **348**, 29 (1995)
27. J. Görres et al.: Phys. Rev. C (submitted and private communication)